

# Inkjet printed conductive polymer-based beam-splitters for terahertz applications

Benjamin S.-Y. Ung,<sup>1,2,\*</sup> Bo Weng,<sup>3</sup> Roderick Shepherd,<sup>4</sup>  
Derek Abbott,<sup>1</sup> and Christophe Fumeaux<sup>1</sup>

<sup>1</sup>*School of Electrical & Electronic Engineering, The University of Adelaide,  
SA 5005, Australia*

<sup>2</sup>*Department of Electronic Engineering, The Chinese University of Hong Kong,  
Shatin, N.T., Hong Kong*

<sup>3</sup>*ARC Centre of Excellence for Electromaterials Science, Intelligent Polymer Research  
Institute, University of Wollongong, NSW 2522, Australia*

<sup>4</sup>*School of Chemical and Biomolecular Engineering, The University of Sydney, Sydney,  
NSW 2006, Australia*

[\\*bung@eleceng.adelaide.edu.au](mailto:*bung@eleceng.adelaide.edu.au)

**Abstract:** Terahertz beam-splitters are fabricated from conductive polymers inkjet printed onto an acetate film substrate. The principle is a significant evolution of the recently proposed ultra-thin beam-splitter realized using silver conductive paint. The splitting ratios of the beam-splitters are dependent on the thickness and conductivity of the conductive polymer layer, allowing for any splitting ratio to be achieved accurately from a controlled printing process. As the processing technology of conductive polymers matures, this approach will allow for low cost and accurate fabrication of THz beam-splitters with a predefined near frequency-independent splitting ratio, in contrast to the commonly used float zone silicon wafers.

© 2013 Optical Society of America

**OCIS codes:** (300.6495) Spectroscopy, terahertz; (040.2235) Far infrared or terahertz; (230.1360) Beam splitters.

---

## References and links

1. H. Shirakawa, E. J. Louis, A. G. MacDiarmid, C. K. Chiang, and A. J. Heeger, "Synthesis of electrically conducting organic polymers: halogen derivatives of polyacetylene, (CH)<sub>x</sub>," *J. Chem. Soc., Chem. Commun.* **16**, 578–580 (1977).
2. A. J. Heeger, S. Kivelson, J. R. Schrieffer, and W. P. Su, "Solitons in conducting polymers," *Rev. Mod. Phys.* **60**(3), 781–850 (1988).
3. A. M. Stoneham, M. M. D. Ramos, A. M. Almeida, H. M. G. Correia, R. M. Ribeiro, H. Ness, and A. J. Fisher, "Understanding electron flow in conducting polymer films: injection, mobility, recombination and mesostructure," *J. Phys—Condens. Matter* **14**(42), 9877–9898 (2002).
4. T.-I. Jeon, D. Grischkowsky, A. K. Mukherjee, and R. Menon, "Electrical characterization of conducting polypyrrole by THz time-domain spectroscopy," *Appl. Phys. Lett.* **77**(16), 2452–2454 (2000).
5. E. Nguema, V. Vigneras, J. Miane, and P. Mounaix, "Dielectric properties of conducting polyaniline films by THz time-domain spectroscopy," *Eur. Polym. J.* **44**(1), 124–129 (2008).
6. B. S.-Y. Ung, C. Fumeaux, H. Lin, B. Fischer, B. W.-H. Ng, and D. Abbott, "Low-cost ultra-thin broadband terahertz beam-splitter," *Opt. Express* **20**(5), 4968–4978 (2012).
7. C. Berry and M. Jarrahi, "Broadband terahertz polarizing beam splitter on a polymer substrate," *J. Infrared Millim. Terahertz Waves* **32**(12), 1–4 (2011).
8. C. C. Homes, G. L. Carr, R. P. S. M. Lobo, J. D. LaVeigne, and D. B. Tanner, "Silicon beam splitter for far-infrared and terahertz spectroscopy," *Appl. Opt.* **46**(32), 7884–7888 (2007).
9. J.-S. Li, D.-G. Xu, and J.-Q. Yao, "Compact terahertz wave polarizing beam splitter," *Appl. Opt.* **49**(24), 4494–4497 (2010).

10. M. Zhang, X. Li, W. Wang, J. Liu, and Z. Hong, "Terahertz polarizing beam splitter based on copper grating on polyimide substrate," *Proc. SPIE, Millimeter-Wave and Terahertz Technologies II* **8562**, 85621S (2012).
11. Y. H. Lo and R. Leonhardt, "Aspheric lenses for terahertz imaging," *Opt. Express* **16**(20), 15991–15998 (2008).
12. B. Scherger, C. Jördens, and M. Koch, "Variable-focus terahertz lens," *Opt. Express* **19**(5), 4528–4535 (2011).
13. B. Scherger, M. Scheller, C. Jansen, M. Koch, and K. Wiesauer, "Terahertz lenses made by compression molding of micropowders," *Appl. Opt.* **50**(15), 2256–2262 (2011).
14. A. Siemion, A. Siemion, M. Makowski, M. Sypek, E. Hérault, F. Garet, and J.-L. Coutaz, "Off-axis metallic diffractive lens for terahertz beams," *Opt. Lett.* **36**(11), 1960–1962 (2011).
15. L. Ren, C. L. Pint, T. Arikawa, K. Takeya, I. Kawayama, M. Tonouchi, R. H. Hauge, and J. Kono, "Broadband terahertz polarizers with ideal performance based on aligned carbon nanotube stacks," *Nano Lett.* **12**(7), 787–790 (2012).
16. Z. Huang, H. Park, E. P. J. Parrott, H. P. Chan, and E. Pickwell-MacPherson, "Robust thin-film wire-grid THz polarizer fabricated via a low-cost approach," *IEEE Photon. Technol. Lett.* **25**(1), 81–84 (2013).
17. S. Atakaramians, S. Asfar V., M. Nagel, H. K. Rasmussen, O. Bang, T. M. Munro, and D. Abbott, "Direct probing of evanescent field characterization of porous fibers," *Appl. Phys. Lett.* **98**(12), 121104 (2011).
18. R. Mendis and D. M. Mittleman, "Comparison of the lowest-order transverse-electric (TE<sub>1</sub>) and transverse-magnetic (TEM) modes of the parallel-plate waveguide for terahertz pulse applications," *Opt. Express* **17**(17), 14839–14850 (2009).
19. K. Nielsen, H. K. Rasmussen, A. J. Adam, P. C. Planken, O. Bang, and P. U. Jepsen, "Bendable, low-loss Topas fibers for the terahertz frequency range," *Opt. Express* **17**(10), 8592–8601 (2009).
20. B. Scherger, M. Scheller, N. Vieweg, S. T. Cundiff, and M. Koch, "Paper terahertz wave plates," *Opt. Express* **19**(25), 24884–24889 (2011).
21. A. Das, T. M. Schutzius, C. M. Megaridis, S. Subhechha, T. Wang, and L. Liu, "Quasi-optical terahertz polarizers enabled by inkjet printing of carbon nanocomposites," *Appl. Phys. Lett.* **101**(24), 243108 (2012).
22. L. Groenendaal, F. Jonas, D. Freitag, H. Pielartzik, and J. R. Reynolds, "Poly(3,4-ethylenedioxythiophene) and its derivatives: past, present, and future," *Adv. Mater.* **12**(7), 481–494 (2000).
23. T. V. Vernitskaya and O. N. Efimov, "Polypyrrole: a conducting polymer; its synthesis, properties and applications," *Russ. Chem. Rev.* **66**(5), 443–457 (1997).
24. M. Yamashita, C. Otani, M. Shimizu, and H. Okuzaki, "Effect of solvent on carrier transport in poly(3,4-ethylenedioxythiophene)/poly(4-styrenesulfonate) studied by terahertz and infrared-ultraviolet spectroscopy," *Appl. Phys. Lett.* **99**(14), 143307 (2011).
25. O. S. Heavens, *Optical Properties of Thin Solid Films* (Butterworth's Scientific Publications, 1955).
26. S. Bauer, "Optical properties of a metal film and its application as an infrared absorber and as a beam splitter," *Am. J. Phys.* **60**(3), 257–261 (1992).
27. I. Pupeza, R. Wilk, and M. Koch, "Highly accurate optical material parameter determination with THz time-domain spectroscopy," *Opt. Express* **15**(7), 4335–4350 (2007).
28. B. Weng, R. Shepherd, J. Chen, and G. G. Wallace, "Gemini surfactant doped polypyrrole nanodispersions: an inkjet printable formulation," *J. Mater. Chem.* **21**(6), 1918–1924 (2011).
29. M. Walther, D. G. Cooke, C. Sherstan, M. Hajar, M. R. Freeman, and F. A. Hegmann, "Terahertz conductivity of thin gold films at the metal-insulator percolation transition," *Phys. Rev. B* **76**(12), 125408 (2007).
30. M. Tinkham, "Energy gap interpretation of experiments on infrared transmission through superconducting films," *Phys. Rev.* **104**(3), 845–846 (1956).
31. B. Ung, A. Mazhorova, A. Dupuis, M. Rozé, and M. Skorobogatiy, "Polymer microstructured optical fibers for terahertz wave guiding," *Opt. Express* **19**(26), B848–B861 (2011).
32. S. Brett Walker and J. A. Lewis, "Reactive silver inks for patterning high-conductivity features at mild temperatures," *J. Am. Chem. Soc.* **134**(3), 1419–1421 (2012).

## 1. Introduction

Conductive polymers have attracted much interest in the scientific community in recent times as materials, which provide a physically flexible layer while being at the same time electrically conductive. This combination of properties opens many avenues for the advancement of research and technology, and this potential has been recognized by the 2000 Nobel Prize in Chemistry awarded to Heeger, MacDiarmid and Shirakawa for their discovery and development of conductive polymers [1]. Although the properties of conductive polymers [2, 3] have been explored in the terahertz frequency range [4, 5], there are as of yet few practical applications for them in this spectral range. In this context, this paper shows a substantial evolution to the previously published work [6], where a terahertz beam-splitter fabricated from a thin conductive layer—thinner than a skin-depth—was demonstrated with predefined splitting ratios and

nearly frequency-independent behaviour over a wide bandwidth. The use of conductive polymers can significantly add capability to this application, and more generally to the development of many terahertz optical devices, which include beam-splitters [7–10], lenses [11–14], polarizers [15, 16] and waveguides [17–20]. A current publication has also demonstrated polarizers for the THz range fabricated using conductive polymers [21].

The work discussed in this paper focuses on two types of well-known conductive polymers, Poly(3,4-ethylenedioxythiophene) (PEDOT) [22] and Polypyrrole (PPY) [23], which exhibit differing DC conductivities, of which PEDOT has previously been measured at THz frequencies [24]. Both materials are deposited on a thin polymer substrate through an inkjet printing technique. Through appropriate adjustment of the conductive polymer thickness beam-splitters with predefined transmission/reflection ratios can be readily realized. The principle is further demonstrated experimentally using two thicknesses of the PEDOT conductive polymer showing the difference in transmittance and reflectance resulting from a change in thickness with a constant DC conductivity. The presented concept has potential for low-cost production of accurate terahertz beam-splitters with wideband, reasonably frequency-independent splitting ratios.

## 2. Theoretical model

The theoretical model to calculate the transmittance  $t^2(\omega)$  of the samples is uses standard Fabry-Pérot equations [25] over air, conductive polymer and substrate layers. The loss  $A(\omega)$  is then calculated according to [26],

$$A(\omega) = \left( \frac{4y}{\tilde{n}} \cos \varphi_0 \right) / \left( 2 + \frac{y}{\tilde{n}} \cos \varphi_0 \right)^2, \quad (1)$$

where  $\tilde{n}$  is the frequency dependent complex refractive index,  $\varphi_0$  the angle of incidence and  $y = (\sigma_0 d) / (\epsilon_0 c)$ , with  $\sigma_0$  the DC conductivity of the conductive polymer,  $d$  the thickness of the conductive polymer,  $\epsilon_0$  the permittivity of vacuum and  $c$  the speed of light [26]. Thus the reflectance  $r^2(\omega)$  can be calculated as  $r^2(\omega) = 1 - [t^2(\omega) + A(\omega)]$ .

The complex refractive indexes of the three samples used in the theoretical model are calculated, by first measuring the samples in transmission mode, then applying the Spatially Variant Moving Average Filter (SVMAF) in the implementation of the commercially available software *Teralyzer* [27]. A curve fit is then applied to the acquired data for both the real and imaginary parts of the frequency-dependent refractive indexes for both the PEDOT and PPY samples. The PEDOT samples use the same refractive index, while the PPY has a different refractive index. The DC conductivities of the PEDOT and PPY are known from fabrication. The behaviour of the samples can then be calculated in the frequency domain as a function of both the angle of incidence and the specific frequency of operation. The predictions from this theoretical model are discussed in Section 5 and compared to the acquired reference, transmittance and reflectance data.

## 3. Fabrication

The PEDOT and PPY samples were fabricated using a Dimatix DMP2800 piezoelectric inkjet printer to deposit successive layers on an optically transparent acetate over-head projector film of 100  $\mu\text{m}$  thickness. Both polymers were processed as aqueous dispersions and were passed through 3.1 micron filters prior to printing to minimise the likelihood of blocked nozzles. For the printing process, CLEVIOS<sup>TM</sup> P Jet HC V2 PEDOT ink was purchased from HC Starck, Germany and the PPY ink was developed in-house specifically for processing with Dimatix piezoelectric printheads [28]. Two thicknesses of PEDOT are fabricated (1 & 2  $\mu\text{m}$ ), while a single 1  $\mu\text{m}$  thick sample of PPY is also fabricated. The fabricated samples can be seen in

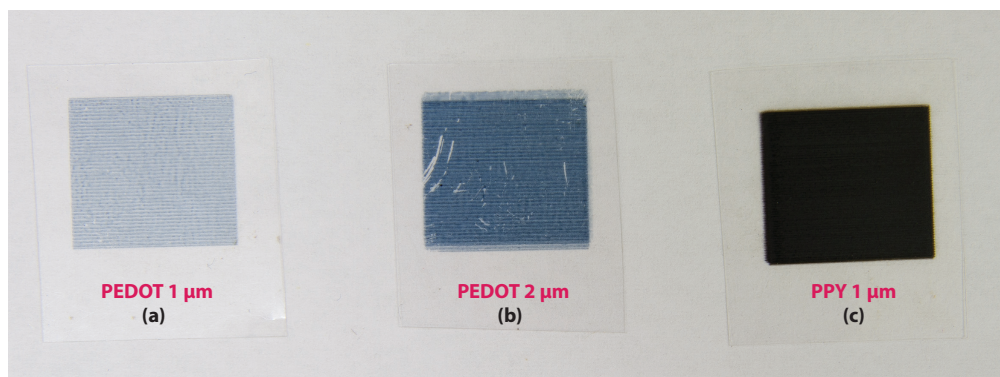


Fig. 1. From left to right, 1  $\mu\text{m}$  and 2  $\mu\text{m}$  thick PEDOT samples and PPY 1  $\mu\text{m}$  in thickness. The conductive polymers are inkjet printed on top of a 100  $\mu\text{m}$  thick acetate overhead projector sheet substrate. The printed squares of conductive polymers have 15 mm side length. The two PEDOT samples show slight non-uniformity, due to the inkjet printing process, and thus appear as an array of striped horizontal lines.

Fig. 1, with the DC conductivities of the PEDOT and PPY being  $\sigma_0 = 160 \text{ S}\cdot\text{cm}^{-1}$  and  $1 \text{ S}\cdot\text{cm}^{-1}$  respectively.

The resulting samples were non-uniform with obvious stripes in the films caused by the inkjet printing procedure employed. Much more uniform films are feasible using these materials and printing process but this would require more optimisation and was beyond the scope of this piece of work. A micrograph taken of the surface of the 1  $\mu\text{m}$  thick PPY sample using a Philips XL40 scanning electron microscope (SEM) in secondary electron detection mode and a beam voltage of 20 kV is shown in Fig. 2. The stripes and gaps from the inkjet printing process can clearly be seen, with widths of approximately 120 and 55  $\mu\text{m}$  respectively.

#### 4. Experimental setup

All reflection and transmission experiments are performed in laboratory atmosphere at room temperature on a Menlo Systems TERA K15, fiber-coupled THz-TDS (terahertz time-domain spectroscopy) system, in the arrangement represented in Fig. 3. The TERA K15 allows for the tight focusing of the THz beam down to approximately 1 mm in diameter via four plano-convex lenses. A customized rotating stage is fabricated to allow for the detector and associated lenses to be swiveled together to the appropriate angle of incidence required by the sample orientation to measure either reflected or transmitted spectra. A sample holder is then mounted on top of the pivoting point of this mechanism. The samples are held in place in this holder using magnets, to ensure that each sample is mounted as flat as possible and that the error due to alignment is minimized when samples are swapped.

All subsequent measurements are performed with a horizontally polarized THz beam, and data is acquired for angles of incidence of  $\varphi_0 = 35^\circ$  to  $55^\circ$ , in  $5^\circ$  increments with a position accurate to  $0.1^\circ$ .

#### 5. Results

The measured transmission and reflection spectra for the different samples are shown in Figs. 4-6 for the three samples considered, and compared to the theoretical model. The left-hand side graphs show the spectral variation of the transmission, reflection and absorption properties, whereas the graphs on the right-hand side illustrate the variations as a function of the angle of

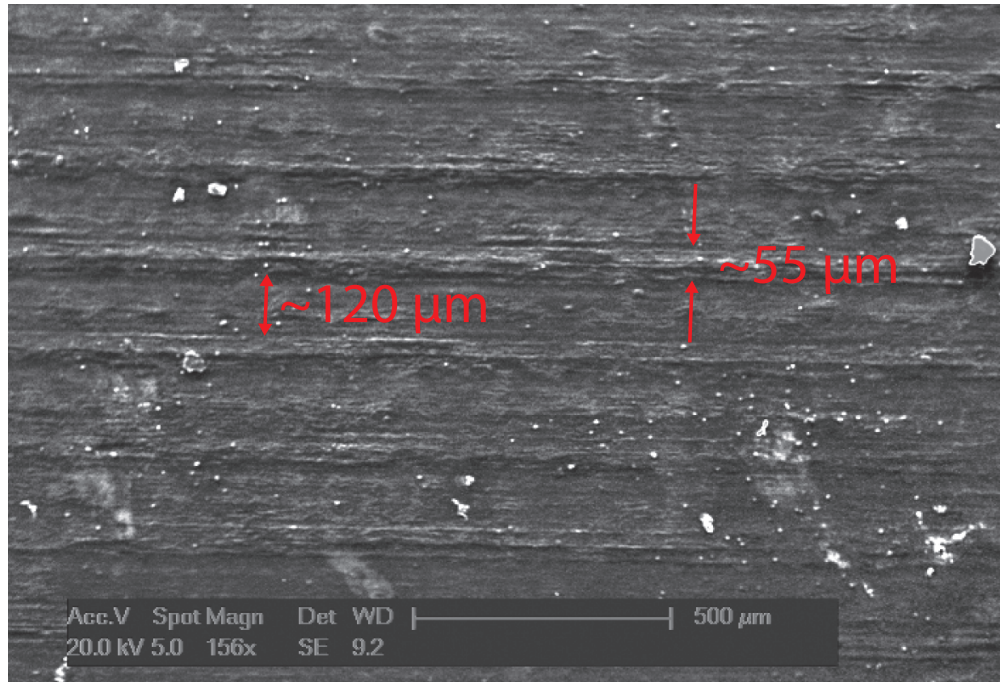


Fig. 2. A SEM micrograph of the surface of the 1  $\mu\text{m}$  thick PPY sample. As with the PEDOT samples, the stripes have a width of approximately 120  $\mu\text{m}$  and gaps between stripes of approximately 55  $\mu\text{m}$ .

incidence, for a fixed frequency of 0.5 THz. The theoretical model obtained *a priori* from the measured refractive index of the samples can be favorably compared to the frequency response of the samples and can predict the performance at varying angles of incidence at a fixed frequency (selected here as 0.5 THz). In particular, the measured data in transmittance shows a close match with the theoretical model for all three samples. In reflectance however, the 1  $\mu\text{m}$  thick PEDOT and PPY samples show a noticeable divergence from the theoretical model at high frequencies. This discrepancy is attributed to the surfaces of the samples not being perfectly optically flat, causing the reflected beam to be partially deflected and scattered away from the detector.

Also shown in Figs. 4–6, the angular measurements from 35° to 55° angles of incidence (in 5° increments) at a frequency of 0.5 THz show a good match with the theoretical model in both the transmittance and reflectance. The transmittance and reflectance increases and decreases respectively as the angle of incidence approaches the Brewster angle near 70°.

The change in thickness of the PEDOT samples from 1 to 2  $\mu\text{m}$  illustrated in Figs. 4 and 5 shows the expected dependence on the layer thickness for a fixed DC conductivity, with the transmittance decreasing and the reflectance increasing for thicker both transmittance and reflectance [6, 29, 30]. Comparing now the 1  $\mu\text{m}$  PEDOT sample to a PPY sample with the same thickness, but lower conductivity, an increase in transmittance and decrease in reflectance is observed, again conforming with theory. The polystyrene substrate itself presents a loss of approximately 5% across the measured frequency range, as well as a minor Fabry-Pérot interference component. Slight misalignment of the the sample in reflection causes losses estimated to be greater than 5% per degree off from the exact angle of incidence. A horizontal or vertical tilting of the sample results in a similar additional loss to the recorded data and therefore, mul-

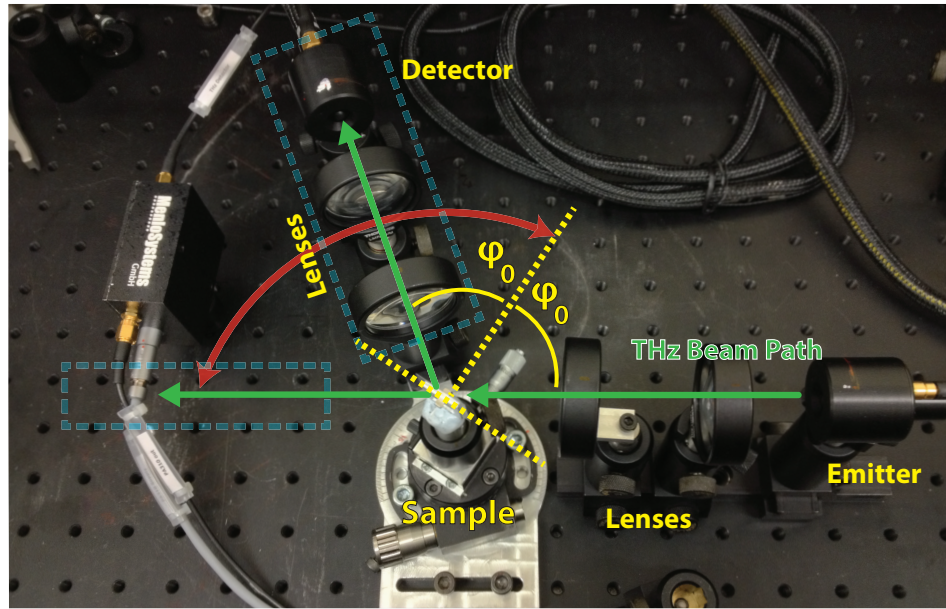


Fig. 3. Photograph of the Menlo Systems THz-TDS system used for measurements. A special sample holder is fabricated, allowing the detector to be swiveled at the appropriate angle to measure both the reflected and transmitted spectra, depending on the angle of incidence on the sample. These positions are highlighted by the blue dashed boxes. The sample is also easily adjusted with a rotational stage accurate to  $0.1^\circ$ .

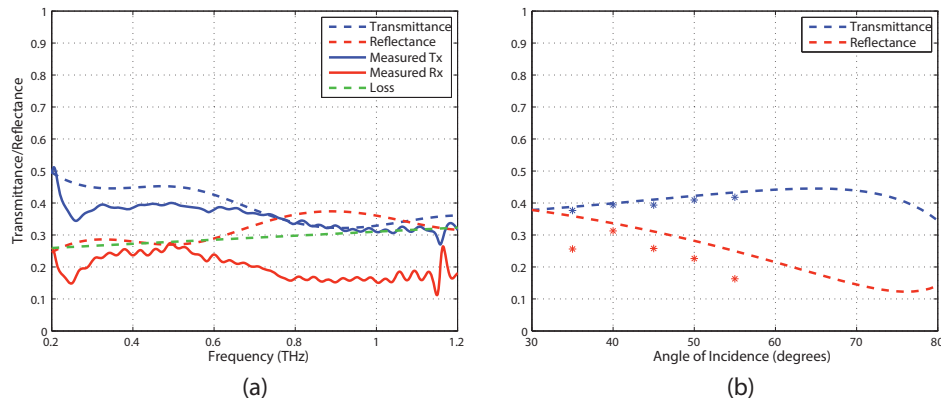


Fig. 4. Transmittance & reflectance plots of the PEDOT  $1 \mu\text{m}$  thick sample. (a) Shows the transmittance & reflectance plot of the sample at  $45^\circ$  incidence, including the calculated loss, while (b) shows the angular dependence of the sample at varying angles of incidence at a fixed frequency of 0.5 THz. (a) Shows a slight variance from the reflectance theoretical model at frequencies above 0.6 THz, due to the non-uniformity of the sample and the substrate not being perfectly optically flat.

multiple measurements are taken to ensure the maximum reflectance is recorded. The effect of the non-uniformity of the film (Fig. 2) can be neglected in a good approximation, as orientating the samples horizontally or vertically in normal incidence transmission mode measurements show

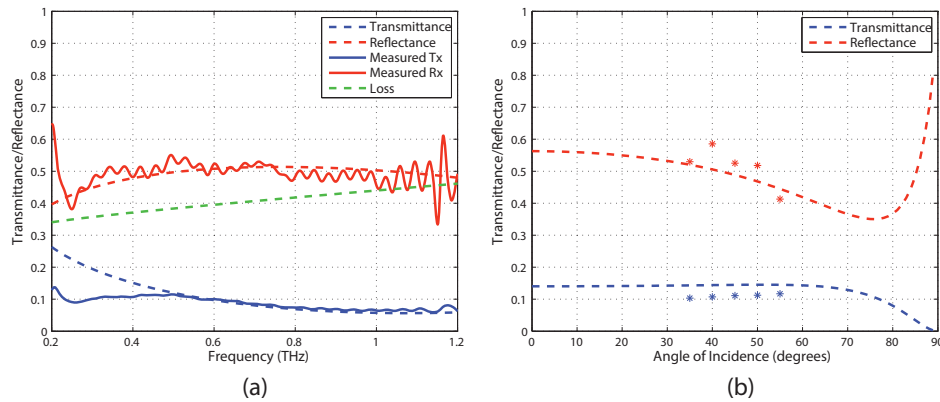


Fig. 5. Transmittance & reflectance plots of the PEDOT 2  $\mu\text{m}$  thick sample. (a) Shows the transmittance & reflectance plot of the sample at  $45^\circ$  incidence, including the calculated loss, while (b) shows the angular dependence of the sample at varying angles of incidence at a fixed frequency of 0.5 THz. The measured data shows good agreement with the theoretical model, however the thicker 2  $\mu\text{m}$  PEDOT coating shows a significantly higher loss than the 1  $\mu\text{m}$  sample.

no significant differences, as shown in Fig. 7.

## 6. Conclusion

The work described in this paper shows that the concept of using thin films of conductive polymers, in particular PEDOT and PPY is promising for realizing beam-splitters in the terahertz range of frequencies. The results from measurements match closely the presented theoretical model, and show the predicted response of the samples in a usable frequency range of 0.2 to 1.2 THz, around the commonly used angles of incidence of  $45^\circ$ . The variations with thickness and conductivity exhibits the same characteristics as demonstrated in previously published work [6], where a conductive layer thinner than the skin depth was used to vary the splitting ratio of a beam-splitter.

The inkjet printing fabrication method of the conductive polymers gives an advantage over previous work, as the resultant thickness is more controllable than other rapid prototyping techniques and can be replicated easily. Further improvements of the printing procedure, or the use of alternative processing procedures such as bar-coating can provide decisive improvements over the proof-of-concept prototypes presented in this investigation to produce uniform coatings. DC conductivities can also be controlled by varying the doping of the polymers, which adds additional control for splitting ratios, if the thickness is to be kept constant. There are some drawbacks to the currently available polymers, as they are not optimized for use at terahertz frequencies. As can be seen from the results, a light Fabry-Pérot interference component is arising from the 100  $\mu\text{m}$  thick substrate, which also partially absorbs the incident terahertz radiation, leading to higher losses. These detrimental effects associated with the substrate could be mitigated by using a very thin substrate of *Teflon*, LDPE (low-density polyethylene) or Topas (cyclic olefin copolymer), all of which show low absorption coefficients up to 3 THz [31]. However changes in the fabrication process are required to achieve this. A further challenge is to keep the free-standing substrate optically flat, as minor changes to the flatness of the surface can cause higher than expected reflection loss through scattering, particularly at higher frequencies. Finally, an alternate possibility for a thin conductive layer coating could be to use the tech-

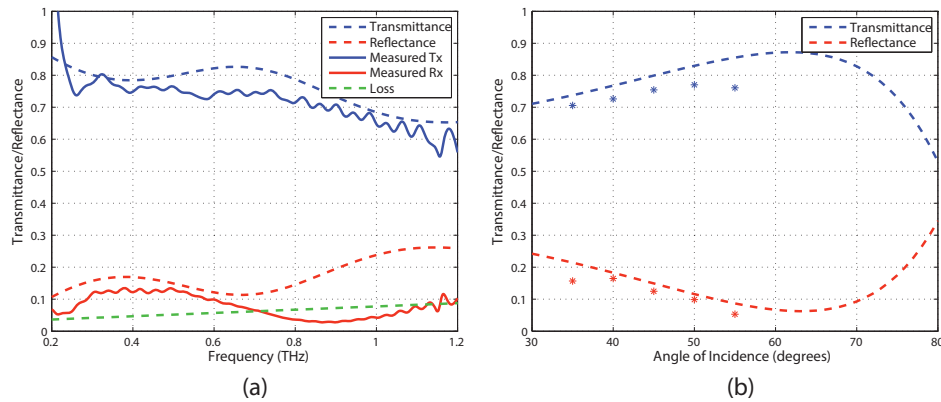


Fig. 6. Transmittance & reflectance plots of the PPY 1  $\mu\text{m}$  thick sample. (a) Shows the transmittance & reflectance plot of the sample at  $45^\circ$  incidence, including the calculated loss, while (b) shows the angular dependence of the sample at varying angles of incidence at a fixed frequency of 0.5 THz. Again, as for the 1  $\mu\text{m}$  PEDOT coating, the 1  $\mu\text{m}$  thick PPY coating show a degradation of the reflectance compared to expectations because of the imperfect flatness of the sample.

niques presented in a recent publication from Walker et al. [32], where metallic inks could be deposited in a similar method to the conductive polymers presented here.

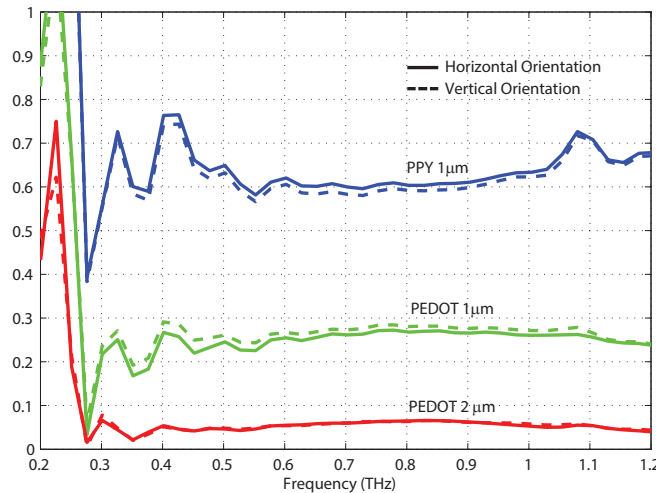


Fig. 7. Normal transmittance measurements of the three samples, PEDOT 1 & 2  $\mu\text{m}$  and PPY in both horizontal and vertical sample orientations (solid and dashed curves respectively). The two differing orientations show no observable differences.

## Acknowledgment

The authors acknowledge funding via the Australian Research Council (ARC) Discovery Projects DP120100661 and DP120100200.